The Journal of the Korean Society of
Coastal and Ocean Engineers
Vol. 1, No. 1, pp. 31~43, December 1989

Tide and Sediment Transport in the Keum River Estuary
錦江河口의 潮汐 및 土砂移動

Byung Ho Choi*, Kyung Gu Kang** and Sok Woo Lee**
崔秉昊*·姜京求**·李錫祐**

Abstract□Tidal asymmetry and the associated sediment dynamics in the Keum River Estuary has been investigated from a numerical tidal model. Modeling efforts were focussed on the simulation of large drying sandflat exposed at the mouth of the Estuary and dynamic combination of two-dimensional estuary model and one-dimensional river model. Despite strong frictional attenuation within the estuary, the M_4 tides reach significant amplitude, resulting in strong tidal distortion. Model results show that the asymmetry over the area exhibit more intense flood flows transport than do less intense ebb flows of longer duration. This causes filling of the estuary as evidenced by large sandflats spread over the inner area. The spatial distribution of peak bottom stress computed from the tidal model suggest that present tidal sedimentation regime may be altered significantly, especially in the approach channel to outer Kunsan port and downstream part of the dike, due to the construction of cross-channel barrier.

要 旨 : 錦江河口의 非線形 潮汐 및 이에 관련된 堆積動力學을 潮汐數値模型을 利用하여 調査하였다. 潮汐模型은 河口潮間帶의 露出樣相 및 二次元 河口模型과 一次元 感潮河川模型을 動的接合시키는 데 力點을 두었다. 模型의 結果는 河口의 强한 摩擦消散에도 불구하고 M_4分潮는 상당한 크기로 算定되었으며 이에 의한 潮汐非線形은 强한 漲潮와 相對的으로 弱하나 持續時間이 긴 落潮로서 提示된 바 河口砂洲形成의 한 要因이 된다. 또한 模型으로부터 算定된 海底最大摩擦應力의 空間的인 分布는 錦江河口둑 建設로 인해 群山港接近水路 및 河口둑 下流部에 큰 堆積變化가 惹起될 수 있음을 提示하고 있다.

1. INTRODUCTION

The Keum River Estuary is a relatively shallow macrotidal embayment (the average tidal range is 5.7 m on springs and 2.8 m on neaps) located at latitude 36 °N of the western coast of Korean Peninsula. Its maximum depth is 10 m (below Indian Spring Low) at the mouth of the estuary (Fig. 1) and it also has a broad intertidal zone, which is about 8 km long, is exposed during low tide. In common with other estuaries in the western coast of Korea, tidal currents have a profound influence on the sediment dynamics in this area. The severe winter storms arising from northwesterly winds also create strong current. Therefore tide and wave conditions of sufficient intensity categorize this area as a high energy environment. The Keum Estuary which have been used by ships entering into the Kunsan inner port and new outer port, is currently subjected to intensive siltation thus seriously limits ships' draft. At present pressures on the port development have led to several studies designed to assess the impact of construction of a cross-channel barrier built 25 km upstream of the Keum River for freshwater storage. These studies, which will have to be devoted as much attention to sediment transport dynamics, require some basic insight into estuarine process. Because of this, hydrodynamical numerical models of tidal flow have an

*成均館大學校 土木工學科(Department of Civil Eng., Sung Kyun Kwan University, Suwon Campus, Suwon, Korea)
**韓國海洋科學技術(株) (Korea Ocean Science and Engineering Corp., Seoul, Korea)

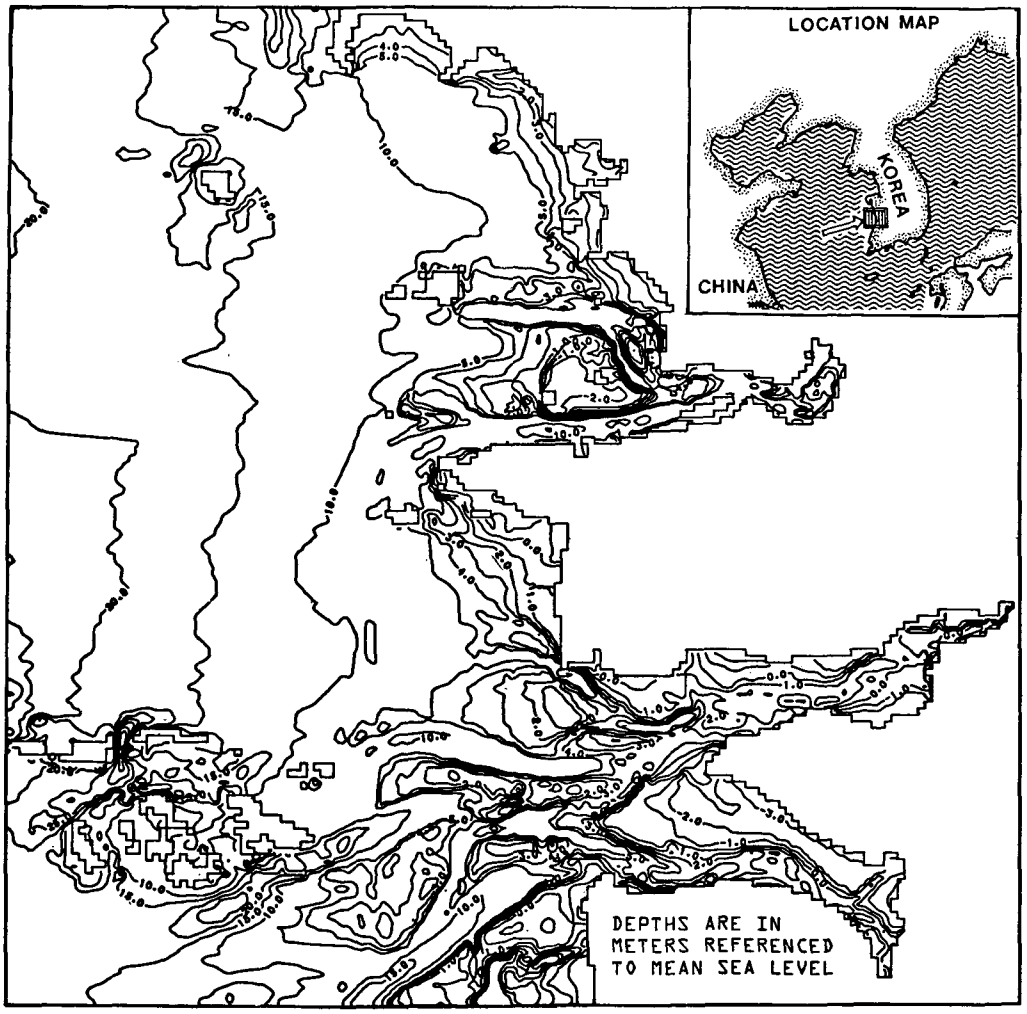

Fig. 1. Bathymetry of Keum River Estuary and vicinity based on Korea Hydrographic Office Charts 322, 336 and coastal development maps from Ministry of Construction.

important role to play in quantifying sediment process in the region. In this paper we will summarize information concerning currents computed from a numerical tidal model adopting dynamical combination of two-dimensional estuary model and one-dimensional river model to investigate the bottom tidal stress and an initial inference on the impact of damming the tidal river on sedimentation regime of the Keum River Estuary.

2. HYDRAULIC REGIME

The Keum River, a 400 km long, with the catchment area of 9,380 km^2 discharges about 70% of its total annual discharge, 6.4×10^9 m^3 during the summer season, July to September (Ministry of Construction, ROK (1974)). The suspended sediment discharge of the Keum River was estimated as about 1.33×10^6 ton/year (Agricultural Development Corporation (1983)) and the bedload may be roughly equivalent to the suspended load. The concentration of suspended sediment in the estuary is quite variable seasonally and on spring-neap cycles. It is about 250-300 mg/l near the mouth on spring tide in dry season. The maximum concentration of 1 to 3 g/l was found about 30 km upstream from the mouth of

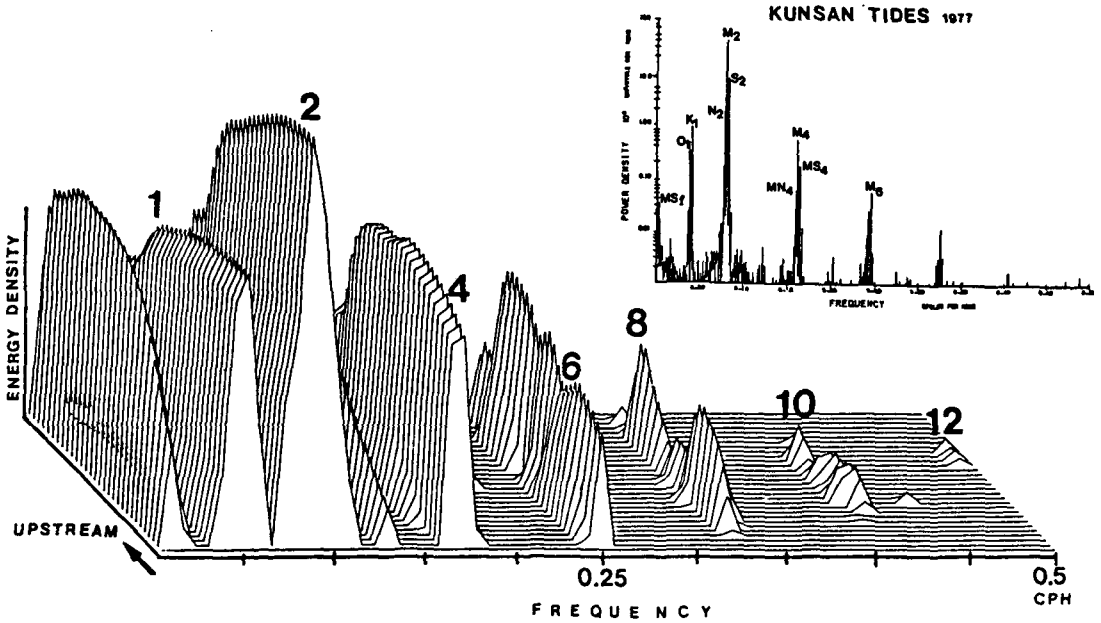

Fig. 2. Sea level spectra at port of Kunsan and its modification along upstream tidal reach. Numbers 1,2,4-refer diurnal, semi- and quarter-diurnal bands.

the estuary in the turbidity maximum (Lee (1984)). In the tidal river residual upstream sediment transport has been reported for strong tide (spring tide) and also with low river discharge, smaller than 2,000 m^3/sec (DHL (1974)). The sediment filtering efficiency of the Keum River was estimated to be 65% (Schubel *et al.* (1984)). The tides enter the Keum Estuary when it propagates northwards along the west coast of Korean Peninsula from the East China Sea continental shelf. Tides at the Keum Estuary are semidiurnal with a diurnal inequality. Neap and spring ranges are 2.8 m and 5.7 m respectively. A power density spectra of observed hourly sea level at permanent tide gauge of Kunsan inner port shows significant contributions of shallow water tides, the ratio of M_4/M_2 amplitude being 0.09. This estuarine tide becomes strongly distorted due to friction, non-linear advection, interaction with channel geometry and freshwater discharge as it propagates into upstream as far as 60 km upstream from the mouth as shown in Fig. 2 (Choi (1987)). Maximum tidal currents average 1.0-1.6 m/sec for spring-neap cycles. The ratio of M_4/M_2 amplitude in tidal current is about 0.2. The flood is shorter but strong throughout the area but reverse situation do occur locally at approach channel to outer port. Tides and tidal currents are about 75° out of phase. Because of strong tidal mixing and low river discharge the estuary is well-mixed (Type C,D) near the entrance and is expected to be partially mixed (Type B) in upper reach where the role of the river relative to tide is greater (Chung (1981)). Fortnightly modulation of daily mean sea level, in phase with the synodic amplitude variation of the tide, has been observed in the tidal reach. Due to this the reversal in the relative levels of MLWS and MLWN is found in upper tidal reach of Ungpo, 24 km upstream from the mouth.

At the mouth of the estuary, Daejuk sandflat is exposed during low tide. Aerial phtograph of this sandflat taken when the tide level is about 70 cm above mean sea level and historial evolution deduced from the series of hydrographic charts and recent surveys are presented in Fig. 3. During the last 80 years changes were noticeable in the movement of horizontal direction and formation of channel in northwest direction.

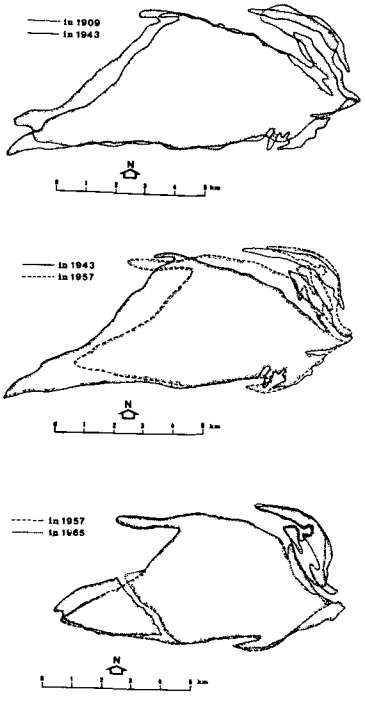

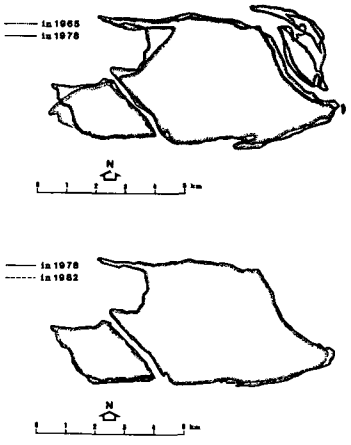

Fig. 3. Aerial photography of Daejuk Sandflats taken on 9 A.M. 22 November 1978 (Courtesy National Geographic Inst. MOC) and historical evolution during the period from 1909 to 1982 (boundaries are referenced to Indian Spring Low).

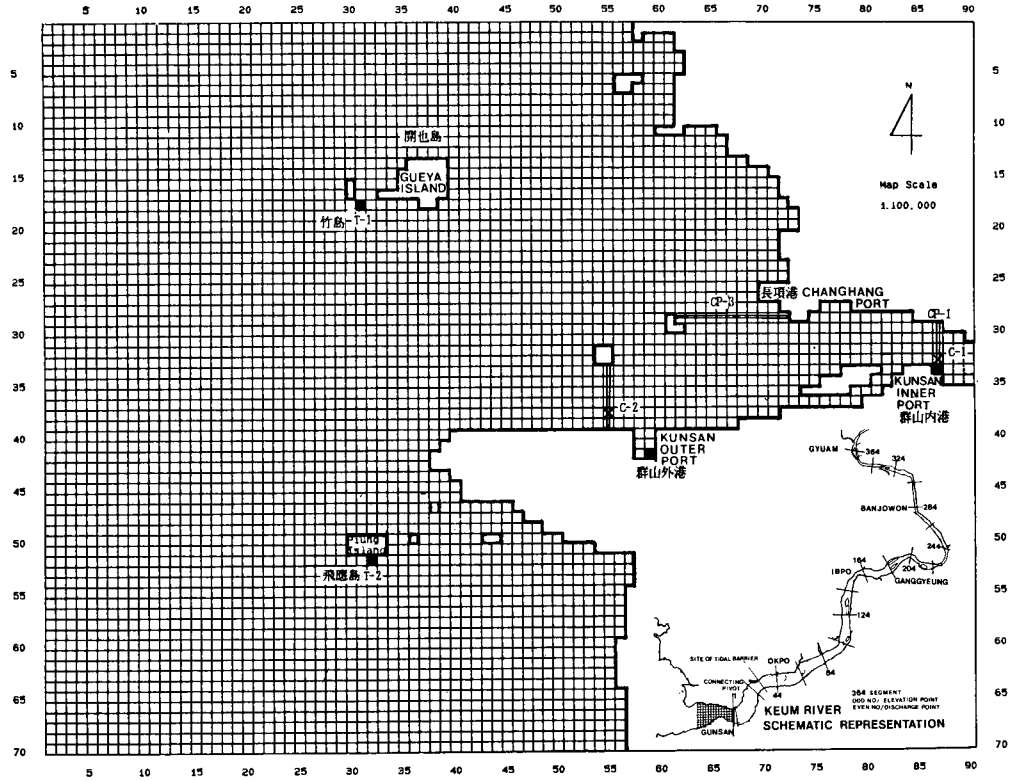

Fig. 4. Finite-difference grid system of two-dimensional Keum Estuary model and segmentations in one-dimensional river model.

3. COMBINATION OF ESTUARY AND RIVER MODELS

An application of hydrodynamical model was attempted to achieve more detailed description of the physical process (both in time and space) than limited observation. The hydrodynamical model uses finite-difference methods to solve the well-known equations of continuity and momentum in their standard non-linear form (Flather & Heaps (1975)). A (90 × 70) lattice of points is used with a uniform spacing of 300 m in two-dimensional estuary model and 364 segments were employed in one-dimensional river model (Fig. 4). A procedure to joining the one- and two-dimensional schemes at the pivot where there is mutual interaction between the motions of the river and the estuary, were carried out through the model calculations. The condition on the water level specified at the seawards boundary are the amplitudes and phases of the M_2 tide to represent average tidal regime. Due to the complex bottom topography of the Keum estuary with the different channel and the sand flats, currents in these areas show great variations depending on the times during the tidal cycle, i.e. whether the sand flats are submerged or not. At low tide currents concentrate in the deeper channels whereas at high tide they spread over the entire area. The accurate representation of the drying sand flats is thus of major importance in solving the problems involved in the sedimentation in the estuary. In the present model the drying sand flats are taken into account by adopting the moving boundary scheme to determine afresh at each timestep the position of the land-sea boundary. Fig. 5 present the results of model simulation showing the exposure and submergence of Daejuk sandflat at intervals of two lunar hours after the passage of the Moon across the local meridian. There are close agreement between the simulation and sand-

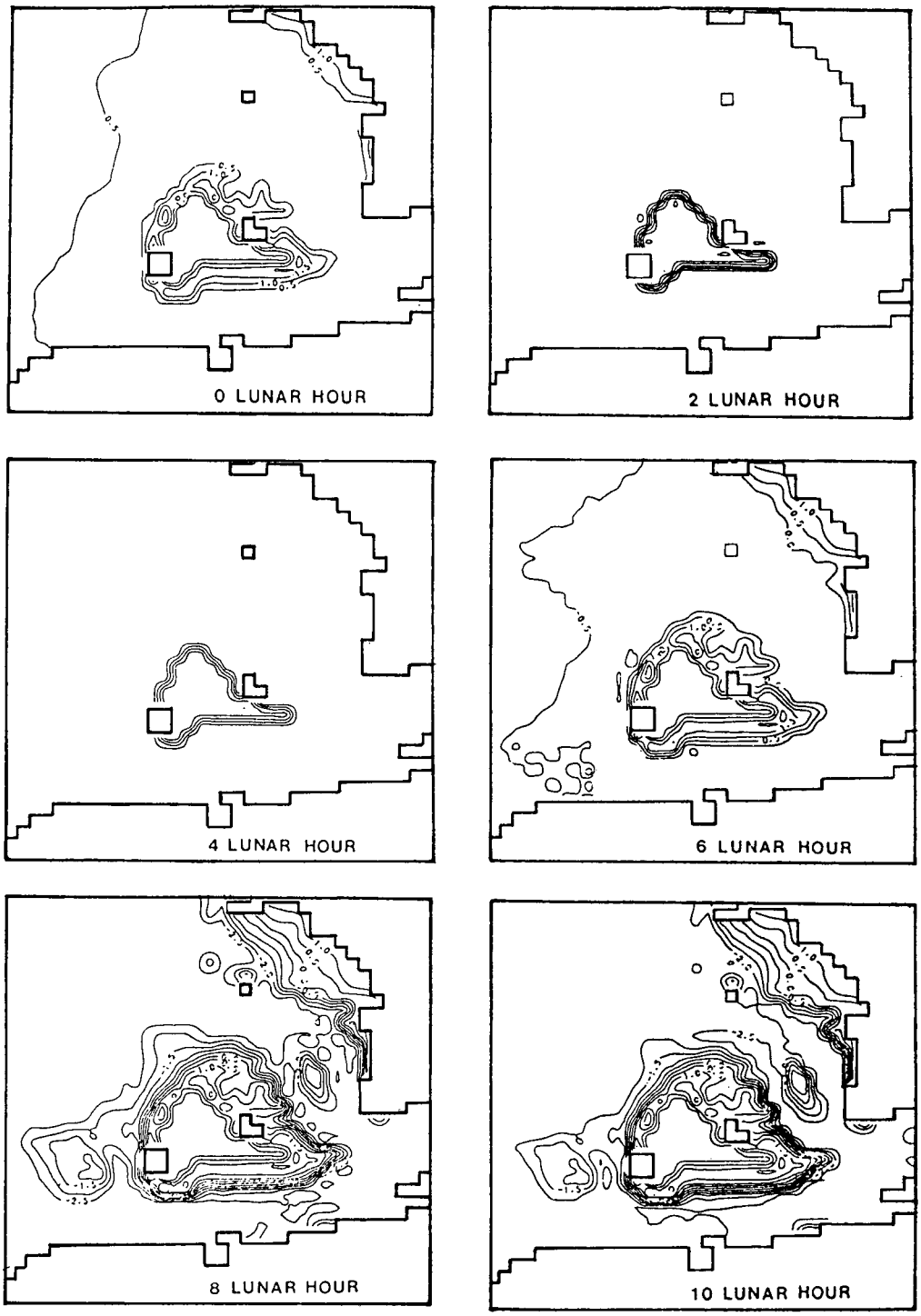

Fig. 5. The spatial distribution of water level and exposure of Daejuk Sandflat computed from the M_2 tidal model shown at intervals of two lunar hours over a cycle.

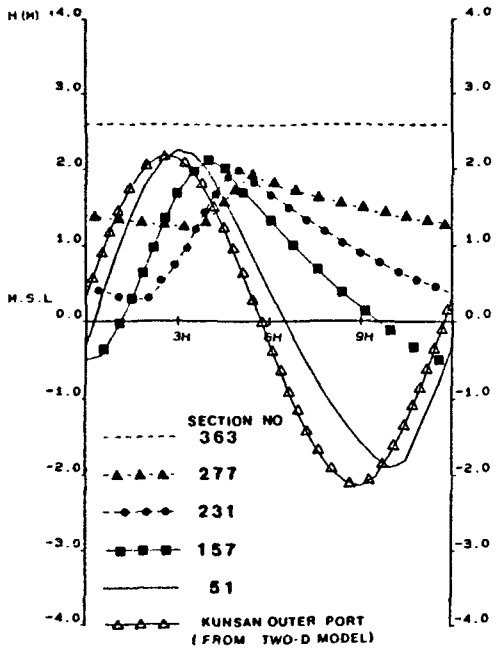

Fig. 6. Computed tides in the river from one-dimensional model.

flat shown in hydrographic charts and LANDSAT images (KORDI (1987)). Generally the amplitudes and phases of the M_2 tidal elevations in good agreement with coastal observations, errors being about 3% in amplitudes and 2° in phases. Fig. 6 show the computed M_2 tide in the tidal reach of the Keum River from the one-dimensional model and there are general agreement between the computation and water level gauge data, thus supporting the joining the one- and two-dimensional schemes. Sets of current vectors also undergo harmonic oscillation and straightforward Fourier analysis was performed to recover the M_2 and overtides from the total disturbances arising due to non-linearities. Thus the resultant velocity vectors describing the M_2 tidal ellipses are shown in Fig. 7. This diagram illustrates an overall impression of the magnitude and direction of the M_2 tidal current distribution representing maximum velocities as semimajor axes. The currents are anticlockwise rotational over the area but elongated ma-

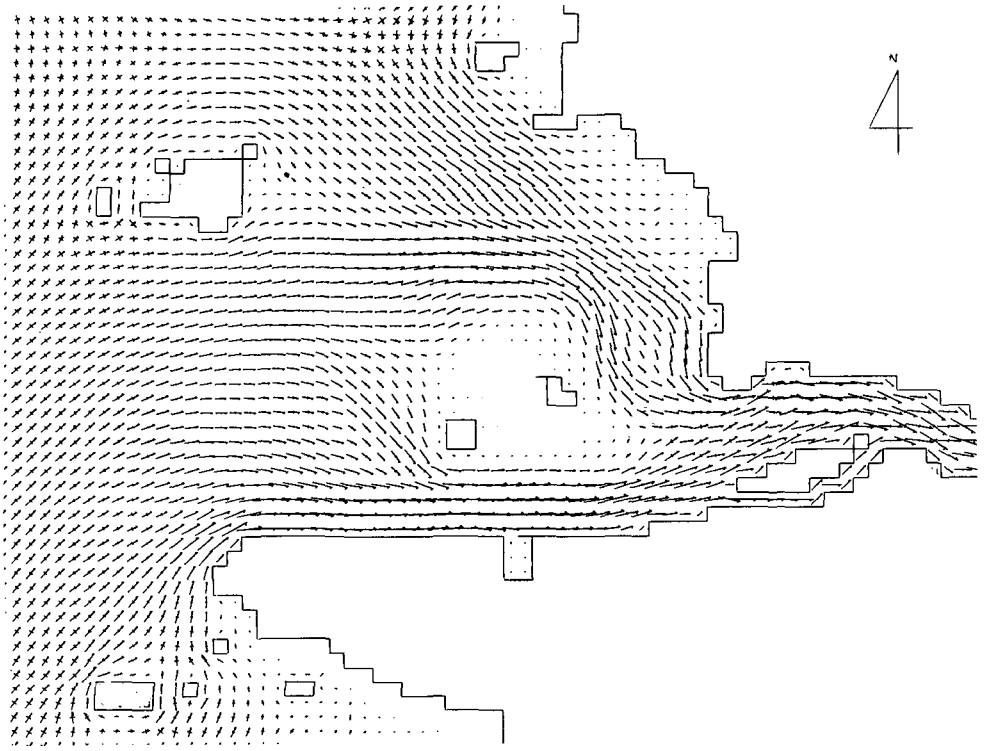

Fig. 7. Computed principal axes of the M_2 tidal ellipses in the Keum River Estuary. Scale of one grid cell equivalent to 1 m/sec.

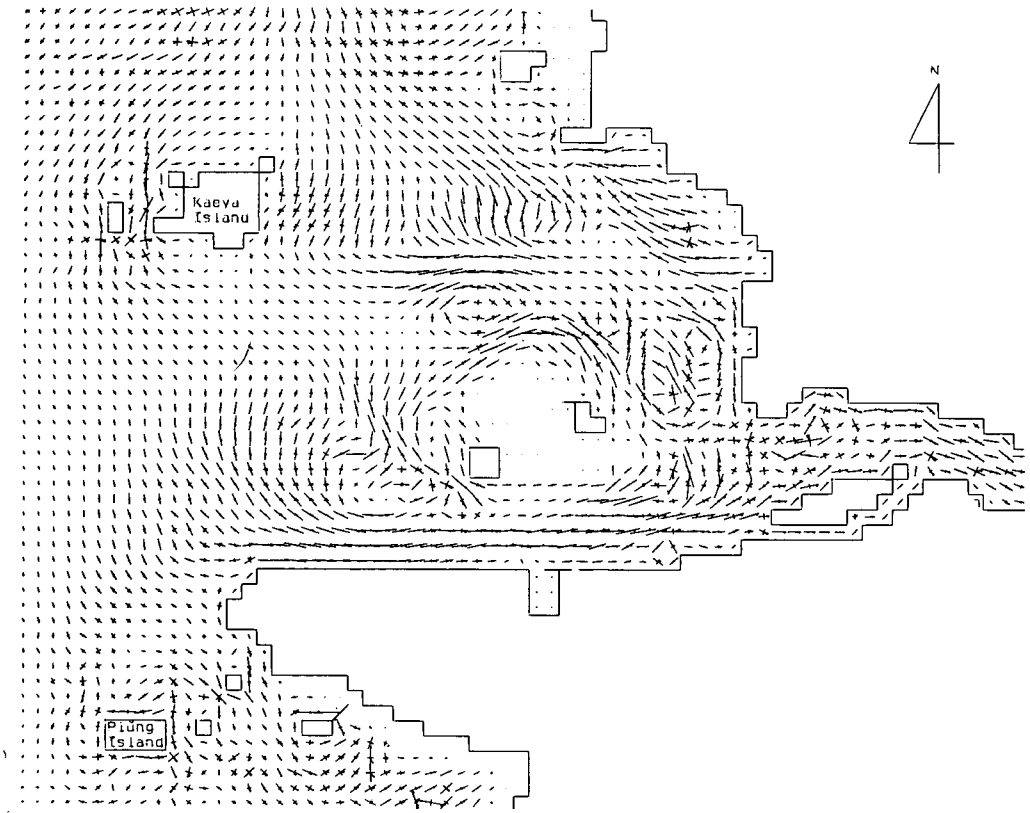

Fig. 8. Computed principal axes of the M_4 tidal ellipses in the Keum River Estuary. Scale of one grid cell equivalent to 0.2 m/sec.

jor axes in the deeper access channels indicate currents are strongly rectilinear. The M_4 currents were also well produced in the channel reflecting local non-linear generation and are shown in Fig. 8 in the form of tidal ellipses. Generally modelled currents were in good agreement with limited observations reproducing the overall hydrodynamic process of the Keum River Estuary.

4. BOTTOM TIDAL STRESS

Using the quadratic formulation, the tidal stress on the sea bed due to frictional drag of water flowing over it may be computed by taking current speed squared times water density times a bottom friction coefficient. Current speed may be used as depth-averaged current from the hydrodynamic model of the Keum Estuary. The strong peak tidal currents ranging from 100 cm/sec to 160 cm/sec in the Keum Estuary may be sufficiently large to cause local resuspension of bedload transport. It has shown that some of key features of the observed sediment transport in the Bristol Channel can be explained in terms of maximum bottom tidal stress (Pingree & Griffiths (1979)) and Uncles (1983)). Fig. 9 shows the distribution of the maximum bottom stress in the Keum River Estuary following the numerical methods of Uncles (1983) which includes the effects of residual flows (Fig. 10) as well as peak stresses due to M_2 and M_4 interactions. In regions of large maximum stress, i.e. access channel in the Keum Estuary, the mean or time-averaged bottom tends to be roughly parallel to maximum stress, although reduced in amplitude. Sternberg *et al.* (1983) estimated that the critical bottom stress needed to initiate sediment movement is roughly 2.0 to 2.2 dyne/cm^2 in the western Yellow Sea where the bed materials are fine sands and silty-clay mud, based on tripod observation. Since the

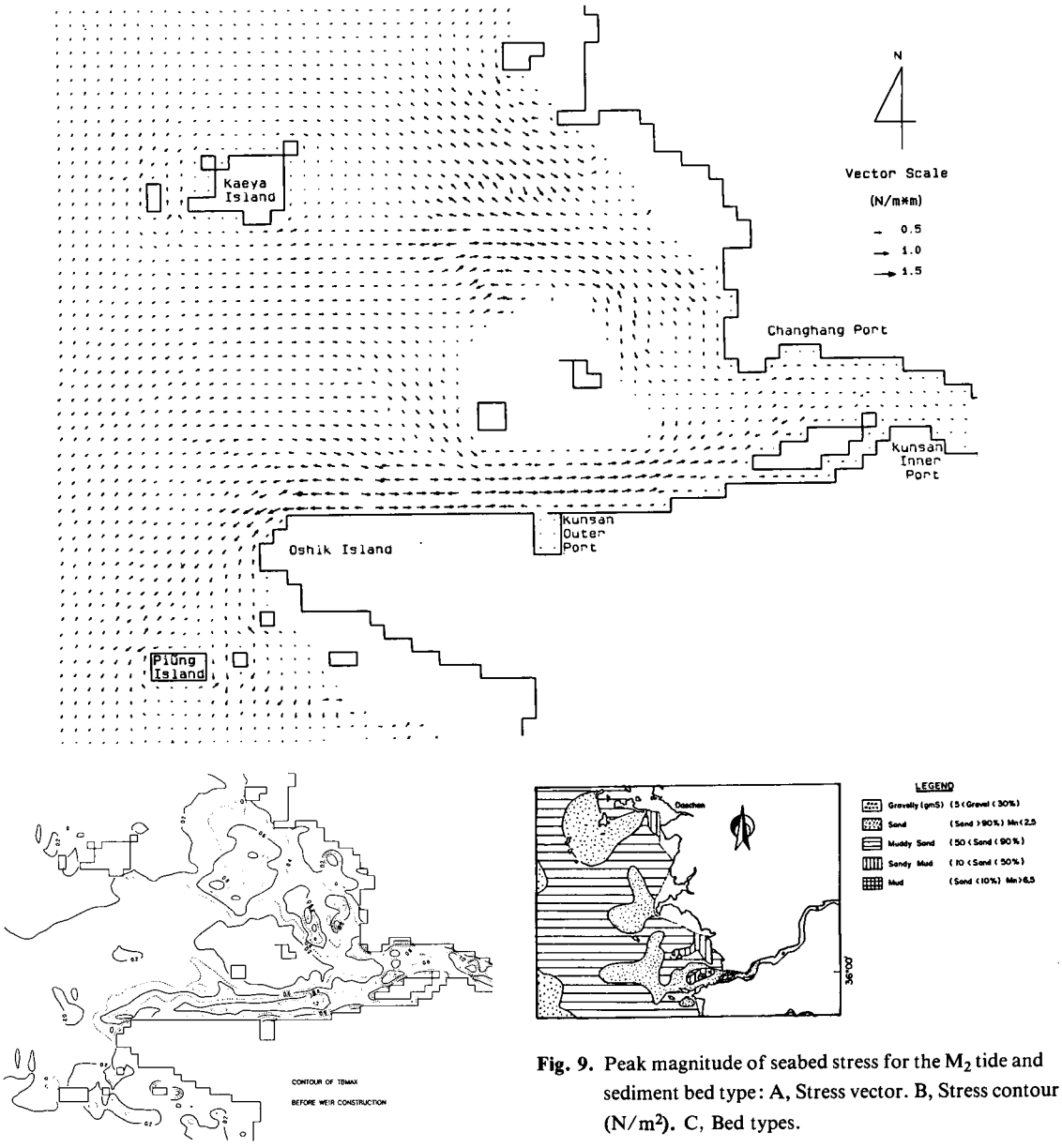

Fig. 9. Peak magnitude of seabed stress for the M_2 tide and sediment bed type: A, Stress vector. B, Stress contour (N/m^2). C, Bed types.

maximum bottom stress exceeds this threshold value by at least a factor of 3-4 over the access channel and inner part of Keum Estuary, tidal currents must play an important role in regional sediment dynamics.

Note that bottom sands in the access channel is associated with high bottom stress in excess of 10 dyne/cm^2 and direction of vectors indicating sediment movement is diverged at the middle part of channel (seawards transport occur in the portion of access channel to outer port and upstream transport in the inner part of the channel). It is also worth noting that delineation of sand flats are characterized by bottom stress contour of about 0.3 N/m^2. As shown in Fig. 10 tidal eddies are associated with sand flats and these secondary circulation effects may also contribute the parmanence of depositions (Heathershaw and Hammond (1980)). Generally the overall direction of stress vectors are shoreward over the

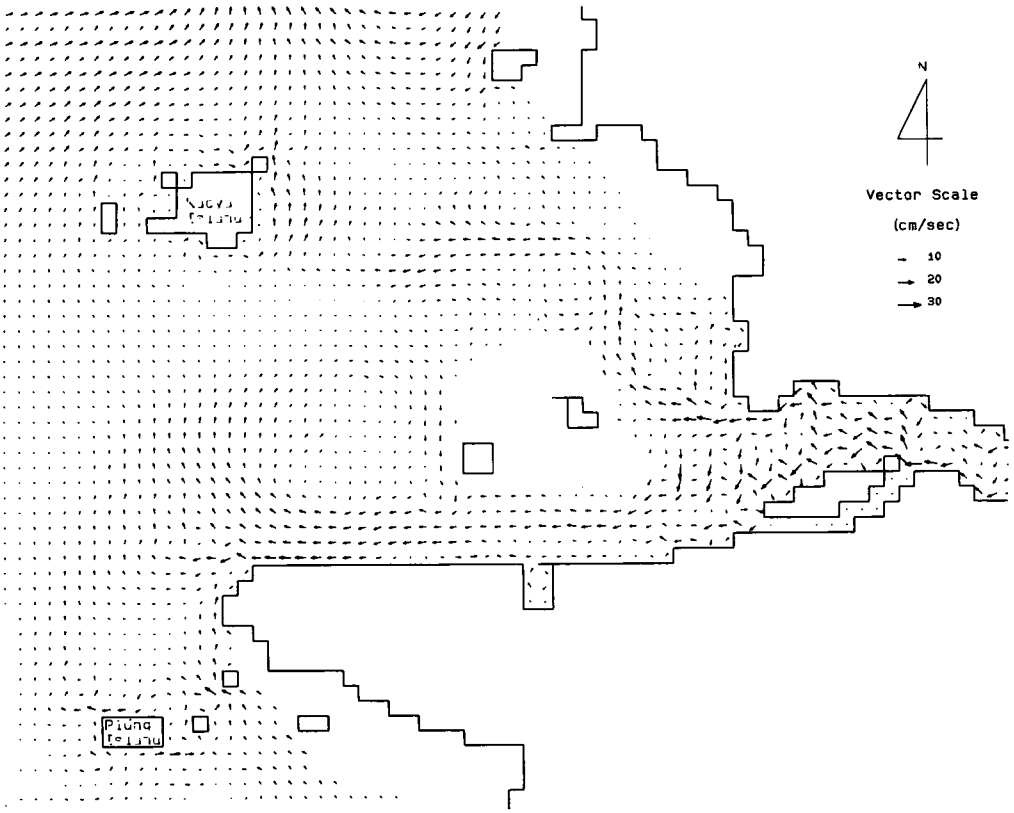

Fig. 10. Eulerian residuals derived from the model and showing anticlock-wise tidal eddies associated with Daejuk sand-flat.

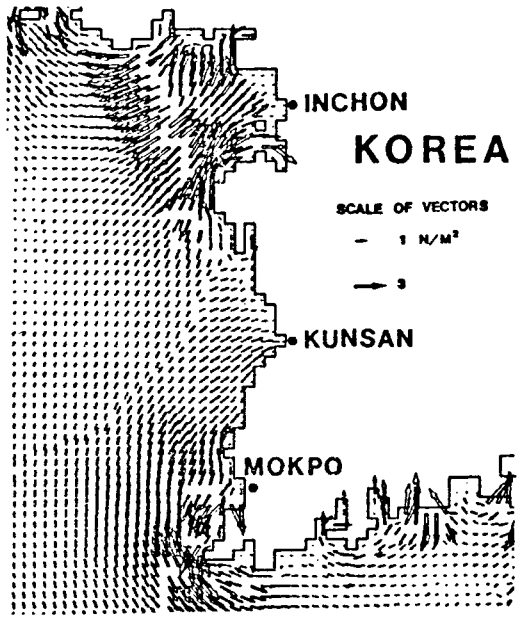

Fig. 11. Distribution of peak bottom stress over the western coast of Korean peninsula (Choi (1988)).

area including the gyre patterns, thus supporting the shoreward transport associated with tidal currents and deposition in the form of sand flats spread over the area. This is further supported by Fig. 11 showing the distribution of maximum bottom stress vectors in the eastern Yellow Sea. The bottom stress field may be reduced as much as by a factor of two due to the reduction in near-bottom M_2 current when a more realistic three-dimensional tidal model is used. The reduced values should still be sufficient to initiate sediment movement, and the sediment transport directions inferred on the basis of the present barotropic two-dimensional model may be reasonable. In the map maximum bottom stress is directed northward from off Mokpo to the Keum Estuary.

The response of the dynamic sedimentation regime to the barrier construction were investigated via the established tidal model. The simulated results show that slight amplication of M_2 tidal elevation in

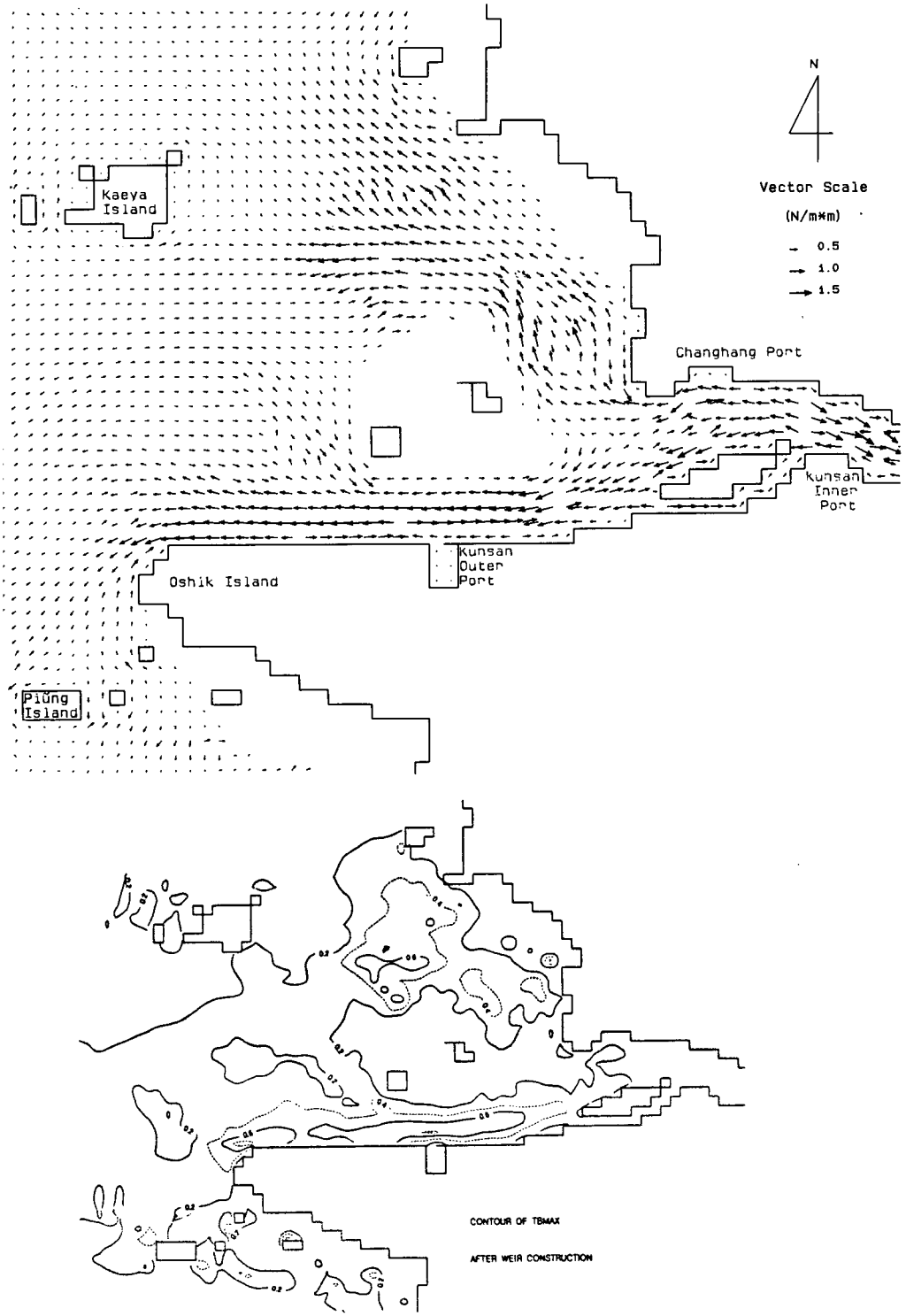

Fig. 12. Predicted peak magnitude of seabed stress for the M_2 tide after the construction of barrier.

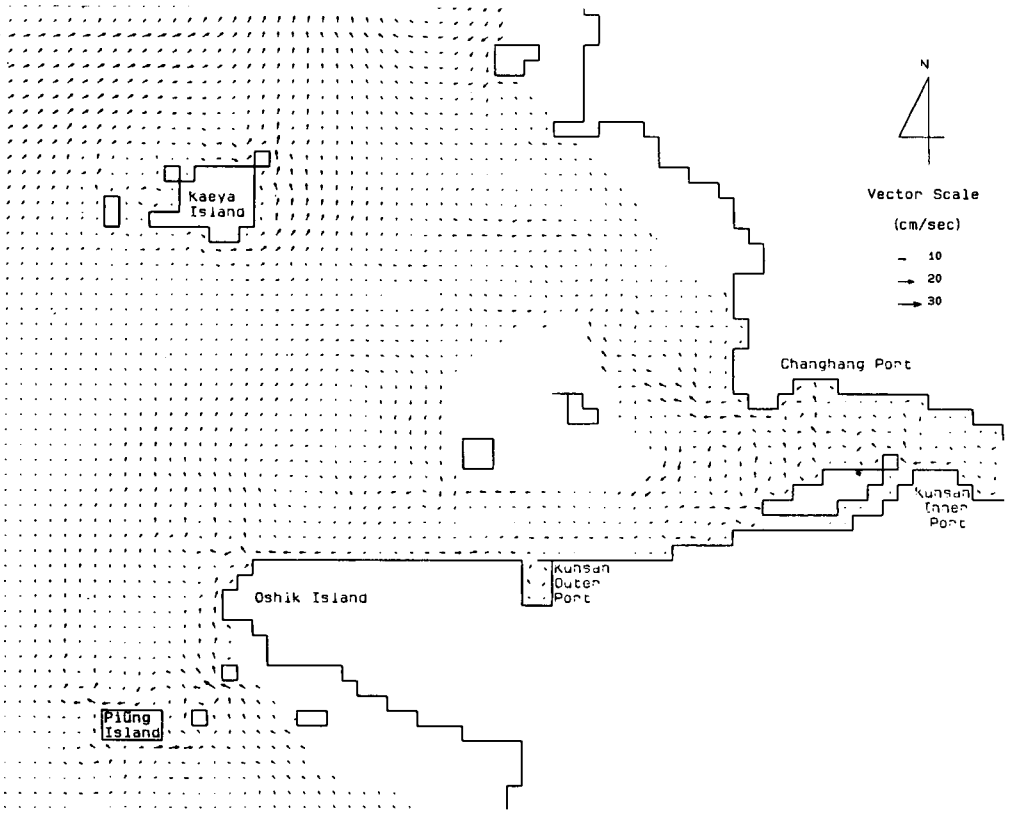

Fig. 13. Eulerian residuals for the M_2 tide after the construction of barrier.

the area adjacent to the downstream side of the barrier and these disturbances are negligible in access channel to outer port. The changes in tidal current regime, however, are very significant. The reduction in current amplitude is about factor of six in the downstream area of the barrier and maximum ebb flow pattern in outer access channel is changed to more intense flood flow condition. These changes are reflected in maps of maximum bottom stress and residual currents as illustrated in Figs. 12 and 13 respectively. It is shown that seaward vectors in the portion of access channel to outer port is changed its direction reversely, thus suggesting the upstream transport will be prevail over the channel. Intensity of bottom stress in downstream area of the barrier is markedly reduced as a consequence of reduction in current intensity. Contour map of bottom stress suggest that there are strong possibility of expanding present sand flats over the area. This initial prediction, by no means indicates more siltation in the channel due to barrier because major sediment supply from the river may be greatly reduced by damming the river. However, the predicted bottom tidal stress may suggest controlling sediment transport mechanism for redistribution of existing bottom sediments and once-discharged sediments through the barrier.

5. CONCLUSION

Accumulation of fine-grain material and sand flats in the Keum River Estuary can be explained by influxes of sediments from outer shelf, sediment from northwest sea area during winter storms, sediment from upstream river and continual resuspension and transport by bottom tidal stress and residual flows. At present there is insufficient knowledge on contribution from individual process to confirm which process is more important. As a first attempt to understand sediment dynamics in the region, inference on the direction of sediment transport as bed-

load and basic mechanism producing this transport which is results of tidal stress and residual flows are performed using a combined one- and two-dimensional hydrodynamical model of tidal flow. Extensive field programme is essential to advance the understanding of sediment dynamics in this estuary. Further modeling effort to incorporate baroclinic process due to river discharge is presently being performed.

REFERENCES

Agricultural Development Corporation, R.O.K., 1983. Environmental impact evaluation on the Keum River area development, Report of ADC, p.389 (in Korean).

Choi, B.H., 1987. Modification of tide in Keum River by river discharge, *Proceedings of Korean Society of Civil Engineers,* Vol. 7, No. 3: 121-131 (in Korean).

Choi, B.H., 1988. A fine-grid two-dimensional M_2 tidal model of the East China Sea, *Journal of Korean Association for Hydrological Sciences,* Vol. 21, No. 3: 183-192.

Chung, J.Y., 1981. Estuarine dynamics of the Keum estuary, Unpublished Report, Seoul National University, Korea (in Korean).

Delft Hydraulic Laboratory, 1974. Fact finding study on sedimentological and salinity intrusion aspects-Ogseo Agricultural Development Project, Vol. 1, Report on Studies, p. 44.

Flather, R.A. and Heaps, N.S., 1975. Tidal computations for Morecambe bay, Geophysical Journal of the Royal Astronomical Society, Vol. 42: 487-517.

Heathershaw, A.D. and Hammond, F.D.C., 1980. Secondary circulation near sand banks and in coastal embayments, Deutsche Hydrographische Zeitschrift, Jahrgang 33, Heft 4: 135-151.

Lee, C.B., 1984. Enrichment and speciation of heavy Metals in the suspended particulated matter of the Keum Estuary, *Proceedings, Korea-U.S. Seminar and Workshop on Marine Geology and Physical Processes of the Yellow Sea:* 182-191.

Korea Ocean Research & Development Institute, 1987. Study on the geomorphology and water turbidity using thematic mapper data of LANDSAT (II): 74 (in Korean).

Ministry of Construction, R.O.K., 1974. Korean Rivers (in Korean).

Pingree, R.D. and Griffiths, D.K., 1979. Sand transport paths around the british isles resulting from M_2 and M_4 tidal interactions, *Journal of Marine Biological Association,* U.K., Vol. 57: 339-354.

Schubel, J.R., Shen, H.T. and Park, M.J., 1984. A comparison of some characteristic sedimentation process of estuaries entering the Yellow Sea, *Proceedings, Korea-U.S. Seminar and Workshop on Marine Geology and Physical processes of the Yellow Sea:* 286-308.

Sternberg, R.W., Larsen, L.H. and Miao, Y.-T., 1983. Near-bottom flow conditions and associated sediment transport on the East China Sea, *Proceedings on the International Symposium on Sedimentation on the Continental Shelf, with Special Reference to the East China Sea,* Vol. 1, China Ocean Press, Beijing: 436-446.

Uncles, R.J., 1983. Modelling tidal stress, circulation and mixing in the bristol channel as a prerequisite for ecosystem studies, *Canadian Journal of Fisheries and Aquatic Sciences* (Supplement), Vol. 40, Supplement No. 1: 8-19.